Ten-channel eikonal treatment of electron–metastable-helium collisions: Differential and integral cross sections for $2^{1,3}P$ and $n=3$ excitations from He ($2^{1,3}S$) and the (λ, χ, Π) parameters*

M. R. Flannery and K. J. McCann
School of Physics, Georgia Institute of Technology, Atlanta, Georgia 30332
(Received 23 April 1975)

We present a ten-channel eikonal treatment of the $2^{1,3}P$, $3^{1,3}S$, $3^{1,3}P$, and $3^{1,3}D$ excitations of atomic helium, initially in the $2^{1,3}S$ metastable states, by incident electrons with energy E (eV) in the range $5 \leq E \leq 100$. Integral and differential inelastic cross sections are obtained. Also, the angular-correlation parameters λ and χ, which respectively provide the relative population and relative phase of the collisionally excited P magnetic substates, and the circular polarization fraction Π of radiation emitted from these P states, are determined as functions of scattering angle θ and E. No measurements exist to date. The principle of detailed balance is explicitly demonstrated for the 2^1S-1^1S superelastic collision.

I. INTRODUCTION

In constrast to collisions involving ground-state atoms, relatively little is known with any great certainty about excitation processes involving atoms initially in a prepared excited state. Such knowledge is very important to the detailed analysis of gaseous discharges, astrophysical plasmas, and formation of excimers[1] (excited metastable molecules, often rare gases).

In this paper, the multichannel eikonal model,[2] which provided a satisfactory account of integral and differential cross sections in e-H($1s$) and e-He($1s^2$) inelastic collisions,[3,4] is applied to the excitation processes

$$e + \mathrm{He}(2^{1,3}S) \rightarrow e + \mathrm{He}(2^{1,3}P, 3^{1,3}S, 3^{1,3}P, 3^{1,3}D). \tag{1}$$

Frozen-core Hartree-Fock wave functions[5] for helium are used throughout, and the $n=1$, 2, and 3 channels of each singlet and triplet series will be closely coupled. In addition to the evaluation of integral and differential cross sections for (1), the angular-correlation parameters λ and χ, which are more basic to the collision process, and which provide valuable information on the circular polarization of the emitted radiation from the $n^{1,3}P$ states, will also be studied as a function of impact energy E and scattering angle θ (in the c.m. frame).

Contrary to that experienced for transitions from ground atomic states, both the Born and the Vainshtein, Presnyakov, and Sobel'man (VPS) approximations predict[1] that collisional excitations from the $2^{1,3}S$ metastable-helium state to the $3^{1,3}D$ and $3^{1,3}S$ (optically forbidden) levels are more probable than excitations to the (optically allowed) $3^{1,3}P$ and $4^{1,3}P$ levels except at incident energies above 100 eV. Hence, couplings between all the states in the $n=2$ and 3 channels are extremely important and require inclusion for a proper treatment of Eq. (1).

II. THEORY

A. Basic approximation

In an effort to clarify more fully the basis of the present approach, an alternative derivation of the multichannel eikonal treatment is instructive. The wave function for the scattering of two (structured) atoms A and B in general, by their mutual interaction $V(\vec{r}, \vec{R})$ at nuclear separation $\vec{R}(X, Y, Z)$, is

$$\Psi_i^+(\vec{r}, \vec{R}) = \psi_i(\vec{r}) e^{i\vec{k}_i \cdot \vec{R}} + \int\int d\vec{r}\,' d\vec{R}\,' G_0^+(\vec{r}, \vec{R}; \vec{r}\,', \vec{R}\,') \times V(\vec{r}\,', \vec{R}\,') \Psi_i^+(\vec{r}\,', \vec{R}\,'), \tag{2}$$

where the two-particle Green's function G_0^+, appropriate to $\mathcal{H}_0$, the Hamiltonian of the unperturbed system of energy E_i at infinite $\vec{R}$, satisfies

$$(E_i - \mathcal{H}_0 + i\epsilon) G_0^+(\vec{r}, \vec{R}; \vec{r}\,', \vec{R}\,') = \delta(\vec{r} - \vec{r}\,')\delta(\vec{R} - \vec{R}\,'), \tag{3}$$

in which the composite internal coordinates are denoted by $\vec{r}$ relative to each parent nucleus. The free-particle Green's function, which propagates the effect of the interaction V at $(\vec{r}\,', \vec{R}\,')$ to $(\vec{r}, \vec{R})$, can be expanded, in terms of the complete set of eigenfunctions of $\mathcal{H}_0$, as

$$G_0^+(\vec{r}, \vec{R}; \vec{r}\,', \vec{R}\,') = \lim_{\epsilon \to 0^+} \frac{1}{(2\pi)^3} \frac{2\mu}{\hbar^2} \sum_n \psi_n(\vec{r}) \psi_n^*(\vec{r}\,') \int \frac{e^{i\vec{k} \cdot (\vec{R} - \vec{R}\,')} d\vec{k}}{k_n^2 - k^2 + i\epsilon}, \tag{4a}$$

with $\psi_n(\vec{r})$ describing the internal structure at infinite nuclear separation $\vec{R}$, where the relative motion is planar with propagation vector $\vec{k}(k_x, k_y, k_z)$. For heavy-particle collisions, and for electron-atom inelastic collisions at intermediate and high impact energy, scattering about the forward direction contributes most to the total cross section,[2-4] and it is therefore a good approximation to assume that the major contributions to the propagator (4a) arise only from those waves at $Z' < Z$ with $k^2 \approx k_z^2$ such that

$$G_0^+(\vec{r},\vec{R};\vec{r}',\vec{R}') = \lim_{\epsilon\to 0^+}\frac{1}{(2\pi)^3}\frac{2\mu}{\hbar^2}\int_{-\infty}^{\infty}e^{ik_x(X-X')}dk_x\int_{-\infty}^{\infty}e^{ik_y(Y-Y')}dk_y\sum_n\psi_n(\vec{r})\psi_n^*(\vec{r}')\left(\int_{-\infty}^{\infty}\frac{e^{ik_z(Z-Z')}}{k_n^2-k_z^2+i\epsilon}dk_z\right)H(Z-Z'), \tag{4b}$$

where $H(Z-Z')$ is the Heaviside step function (unity for $Z' < Z$ and zero otherwise). Hence, by contour integration, and with introduction of the impact parameter $\rho(X, Y)$,

$$G_0^+(\vec{r},\vec{R};\vec{r}',\vec{R}') = \frac{i\mu}{\hbar^2}\sum_s\frac{e^{ik_s(Z-Z')}}{k_s}\delta(\vec{\rho}-\vec{\rho}') \times H(Z-Z')\psi_s(\vec{r})\psi_s^*(\vec{r}'). \tag{4c}$$

The reduction of (4a) to (4c) can also be obtained by the method of stationary phase (cf. Schiff[6] and Gerjuoy and Thomas[7]). *The multichannel eikonal approximation* follows by setting

$$\Psi_i^+(\vec{r},\vec{R}) = \sum_m A_m(\vec{\rho}, Z)\psi_m(\vec{r})e^{iS_m(\vec{R})}, \tag{5}$$

where the eikonal S_m for the relative motion in excitation channel m under the static interaction

$$V_{nm}(\vec{R}) = \langle\psi_n(\vec{r})|V(\vec{r},\vec{R})|\psi_m(\vec{r})\rangle \tag{6}$$

with $n = m$, satisfies

$$(\nabla S_m)^2 - i\hbar(\nabla^2 S_m) = k_m^2 - (2\mu/\hbar^2)V_{mm} \equiv \kappa_m^2(\vec{R}) \tag{7}$$

exactly. The Green's function corresponding to (5) is (4c), with k_s replaced by the *local* wave number κ_s, and hence, (2) with (5) reduces to

$$\Psi_i^+ = \psi_i(\vec{r})e^{iS_i(\vec{R})} - \frac{i\mu}{\hbar^2}\sum_s\int_{\vec{R}'}\frac{e^{i\kappa_s(Z-Z')}}{\kappa_s}\psi_s(\vec{r})\delta(\vec{\rho}-\vec{\rho}')H(Z-Z')\sum_{m\neq s}{}'A_m(\vec{\rho}', Z')V_{sm}(\vec{R}')e^{iS_m(\vec{R}')}d\vec{\rho}'dZ'. \tag{8}$$

The projection of (8) onto the orthonormal set $\psi_n(\vec{r})$ is

$$(A_n e^{iS_n} - \delta_{ni}e^{iS_i})e^{-i\kappa_n Z} = -\frac{i\mu}{\hbar^2}\int_{-\infty}^{Z}\frac{e^{-i\kappa_n Z'}}{\kappa_n(\vec{\rho}, Z')}\sum_m{}'A_m(\vec{\rho}, Z')V_{nm}(\vec{\rho}, Z')e^{iS_m(\vec{\rho},Z')}dZ', \tag{9}$$

which on differentiation yields

$$\frac{\partial}{\partial Z}(A_n e^{i(S_n-\kappa_n Z)}) = -\frac{i\mu}{\kappa_n\hbar^2}\sum_m{}'A_m(\vec{\rho}, Z)V_{nm}(\vec{R})e^{i(S_m(\vec{R})-\kappa_n Z)}. \tag{10}$$

Ignoring the second term on the left-hand side of (7) and assuming a straight-line trajectory along the Z axis, i.e., $|\nabla S_n| \approx \partial S_n/\partial Z \approx \kappa_n$, and $\partial\kappa_n/\partial Z \approx 0$ [equivalent to the neglect of $\nabla^2 S_n$ in (7)], Eq. (10) becomes

$$\frac{i\hbar^2}{\mu}\kappa_n\frac{\partial A_n}{\partial Z} = \sum_{m\neq n}{}'A_m(\vec{\rho}, Z)V_{nm}(\vec{R})e^{i(S_m-S_n)}, \tag{11}$$

a set of first-order coupled differential equations to be solved for A_n. Thus, for a finite number of states $n = 1, 2, \ldots, N$, the direct transition matrix element T_{fi} or its associated scattering amplitude f_{if} can be evaluated from

$$T_{fi} = \langle\psi_f(\vec{r})e^{i\vec{k}_f\cdot\vec{R}}|V(\vec{r},\vec{R})|\sum_n A_n\psi_n(\vec{r})e^{iS_n(\vec{R})}\rangle_{\vec{r},\vec{R}} \equiv -4\pi\frac{\hbar^2}{2\mu}f_{if}(\vec{k}_i,\vec{k}_f) \tag{12a}$$

$$= \sum_n\langle e^{i\vec{k}_f\cdot\vec{R}}|V_{fn}(\vec{R})|A_n(\vec{\rho}, Z)e^{iS_n(\vec{R})}\rangle_{\vec{\rho},Z}, \tag{12b}$$

the basis of the multichannel eikonal treatment.[2] The transition matrix for rearrangement collisions between the projectile at $\vec{R}$ and a target electron at $\vec{r}_i$ is obtained from (12a) by the $\vec{R} \leftrightarrow \vec{r}_i$ interchange in the wave function for the final state f.

The above derivation therefore shows that the multichannel eikonal treatment is based on the following three assumptions: (a) the Green's function (4c), (b) $|\nabla S_n| = \kappa_n$, and (c) a straight-line trajectory used to find the eikonal S_n, all included within a restricted basis set of N target states.

B. Basic formulas

For a nondegenerate initial state i, the experimental differential cross section for $i \to f$ excitation is, as a function of scattering angle θ,

$$\frac{d\sigma}{d\Omega} = \frac{k_f}{k_i} \sum_{M=-L}^{L} |f_{if}^{(M)}(\theta)|^2 , \tag{13}$$

summed over all degenerate magnetic sublevels M of the final level f of the target with angular momentum L, thereby suppressing all knowledge of the populations and phases of each substate. However, two quantities capable of measurement[8] and calculation as functions of θ and impact energy E, can be defined for excitation of the $n^{1,3}P$ levels, by

$$\lambda = |f_{if}^{(0)}|^2 / (|f_{if}^{(0)}|^2 + 2|f_{if}^{(1)}|^2) \tag{14}$$

and

$$\chi = \alpha_1 - \alpha_0 , \tag{15}$$

where α_M is the phase of the scattering amplitude

$$f_{if}^{(M)} = |f_{if}^{(M)}| e^{i\alpha_M} \tag{16}$$

and where the axis of quantization of the target is taken along the incident Z direction defined by $\hat{k}_i$. The parameter λ is the relative contribution arising from the $M=0$ sublevel to (13), while χ is a measure of the coherence between the excitations of the $M=0$ and 1 sublevels, i.e., the phase difference between the corresponding oscillating and rotating dipoles, respectively. A related quantity is therefore the circular-polarization fraction of the radiation emitted from the $n^{1,3}P$ levels in a direction perpendicular to the (assumed) XZ plane of the scattering,

$$\Pi = -2[\lambda(1-\lambda)]^{1/2} \sin\chi \equiv \langle \Delta L_y \rangle , \tag{17}$$

where $\langle \Delta L_y \rangle$ is the expectation value of the angular momentum transferred in the Y direction during the collision.[9]

The basic formula (12) for the scattering amplitude can be further reduced for two-particle interactions for which $V_{fi}(\vec{R}) = V_{fi}(\rho, Z) e^{i\Delta\Phi}$, to yield[2]

$$f_{if}(\theta, \phi) = -i^{\Delta+1} \int_0^\infty J_\Delta(K'\rho) \times [I_1(\rho, \theta) - i\, I_2(\rho, \theta)] \rho\, d\rho , \tag{18}$$

where J_Δ are Bessel functions of integral order, $(M_i - M_f)$ the change in magnetic quantum number, and where K' is the XY component $k_f \sin\theta$ of the momentum change $\vec{K} = \vec{k}_i - \vec{k}_f$. The collision functions

$$I_1(\rho, \theta; \alpha) = \int_{-\infty}^{\infty} \kappa_f(\rho, Z) \left(\frac{\partial C_f(\rho, Z)}{\partial Z} \right) e^{i\alpha Z} dZ \tag{19}$$

and

$$I_2(\rho, \theta; \alpha) = \int_{-\infty}^{\infty} [\kappa_f(\kappa_f - k_f) + (\mu/\hbar^2) V_{ff}] \times C_f(\rho, Z) e^{i\alpha Z} dZ \tag{20}$$

contain a dependence on the scattering angle θ via

$$\alpha = k_f(1 - \cos\theta) = 2k_f \sin^2(\theta/2), \tag{21}$$

the difference between the Z component of the momentum change K and the minimum change $k_i - k_f$ in the collision. The coupling (phase Φ-independent) amplitudes C_f are solutions of the following set of N coupled differential equations

$$\frac{i\hbar^2}{\mu} \kappa_f(\rho, Z) \frac{\partial C_f(\rho, Z)}{\partial Z} + \left(\frac{\hbar^2}{\mu} \kappa_f(\kappa_f - k_f) + V_{ff}(\rho, Z) \right) C_f(\rho, Z) = \sum_{n=1}^{N} C_n(\rho, Z) V_{fn}(\rho, Z) \exp i(k_n - k_f) Z, \quad f = 1, 2, \ldots, N, \tag{22}$$

solved subject to the asymptotic boundary condition $C_f(\rho, -\infty) = \delta_{if}$.

III. RESULTS AND DISCUSSION

In order to express the interaction matrix elements (6) as analytical functions of $\vec{R}$, it proves convenient to transform the frozen-core Hartree-Fock wave functions of Cohen and McEachran.[5] Thus, the spatial wave functions for the $n=1$–3 states of helium are

$$\psi_{1s,nlm}(\vec{r}_1, \vec{r}_2) = N_{nl}[\phi_0(\vec{r}_1)\phi_{nlm}(\vec{r}_2) \pm \phi_0(\vec{r}_2)\phi_{nlm}(\vec{r}_1)], \tag{23}$$

in which the ± signs refer to the symmetric (singlet) and antisymmetric (triplet) cases, respectively. The frozen, inner 1s orbital is (in a.u.)

$$\phi_0(\vec{r}) = 2^{5/2} e^{-2r} Y_{00}(\hat{r}), \tag{24}$$

and the orbital for the second electron in state (nlm) is rewritten (in a.u.) as

$$\phi_{nlm}(\vec{r}) = \sum_{N=l+1}^{J-1} B_N^{nl} e^{-\beta r} r^{N-1} Y_{lm}(\hat{r}), \quad \beta = 2/n , \tag{25}$$

where J is the maximum number of linear coefficients B_N^{nl} given in terms of Cohen and McEachran's original parameters a_j^{nl} by[3]

$$B_N^{nl} = \sum_{j=N+l}^{J} \frac{(-1)^{N-l} 2^l (j!)^2 (2\beta)^{N-l-1}}{(N-l-1)!\,(j-N-l)!\,(N+l)!}\, a_j^{nl},$$

$$N = 1, 2, \ldots, J. \quad (26)$$

The above transformation (26) facilitates subsequent evaluation of the e-He interaction matrix elements

$$V_{ij}(\vec{R}) = \langle \phi_i(\vec{r}_1, \vec{r}_2) | -\frac{2}{R} + \frac{1}{|\vec{R}-\vec{r}_1|} + \frac{1}{|\vec{R}-\vec{r}_2|} | \phi_j(\vec{r}_1, \vec{r}_2) \rangle \quad (27)$$

as analytical functions of $\vec{R}$, for all combinations of i and j appropriate to a ten-state treatment. In addition to the $n=2$ and $n=3$ channels, the superelastic $1\,^1S$ channel was included for singlet-singlet transitions. The above frozen-core approximation for He implies that correlation effects between the inner and outer atomic electrons have been explicitly neglected [although some implicit account is assumed by virtue of (25)], and is therefore effectively exact for highly excited Rydberg states. Metastable helium is unique in that its excitation energy, 19.8 eV above the ground state, is the largest of all the singly excited atoms, its outer electron is relatively weakly bound (~4.8 eV), and the mean interelectronic separation in the $2\,^1S$ state is $\sim 5.3 a_0$. Therefore, the main response of target helium to the projectile electron is expected to arise from the outer electron such that the use of a frozen-core orbital for the inner electron within a close-coupling scattering wave function (5) is expected to be quite accurate. This is further supported by the fact that the dominant contributions to the integral inelastic cross sections for singly excited transitions arise from small scattering angles $\theta \leq 20°$ (cf. Fig. 5) which result from distant encounters. At the lowest impact energy (5 eV), however, the angular distribution tends to become more isotropic such that close encounters are gaining in relative importance. This situation is difficult to assess without resort not only to correlated atomic wave functions, but also to a more elaborate scattering formalism involving some mechanism which permits response of the inner electron to the projectile. If correlation effects with the inner electron are to be included in the atomic function, then similar refinements involving its interaction with the projectile must also be included in a more elaborate scattering formalism, not based on an atomic close-coupling expansion valid only for weak perturbations, but on some perturbed three-body expansion. It is worth noting that the atomic wave functions adopted in this paper are the most accurate ones used to date in any scattering description more refined than Born's approximation.

In Figs. 1–3 are displayed the integral cross sections for the processes

$$e + \mathrm{He}(2\,^{1,3}S) \rightarrow e + \mathrm{He}(2\,^{1,3}P, 3\,^{1,3}S, 3\,^{1,3}P, 3\,^{1,3}D) \quad (28)$$

at incident-electron energies E (eV) in the range $5 \leq E \leq 100$, together with comparison Born values determined from the highly accurate form factors of Kim and Inokuti.[10] It is worth noting that the coupled-state calculations were much more time consuming (~5 h U1108) than a corresponding treatment of excitation from the ground state[3,4] which involved ~1 h U1108. This additional time resulted from the closeness of the initial $2\,^1S$ with neighboring $2\,^1P$ channels which, because of their long-range static and coupled interactions, necessitated the inclusion of large impact parameters $\rho \sim 100$ a.u. in order to achieve convergence for both the solutions of the coupled equations (22) and for the integration (18) involving the Bessel functions which oscillated rapidly at these large ρ.

In general, transitions between singlet states of given configurations are much more probable than the corresponding triplet-triplet transitions. Figs. 1–3 show that the multichannel treatment preserves the Born predictions of the relative importance of transitions to the $2\,^{1,3}P$, $3\,^{1,3}D$, $3\,^{1,3}S$, and $3\,^{1,3}P$ states, written in order of decreasing probability, except at $E \gtrsim 25$ eV and $\gtrsim 70$ eV when excitations of the $3\,^1P$ and $3\,^3P$ states, respectively,

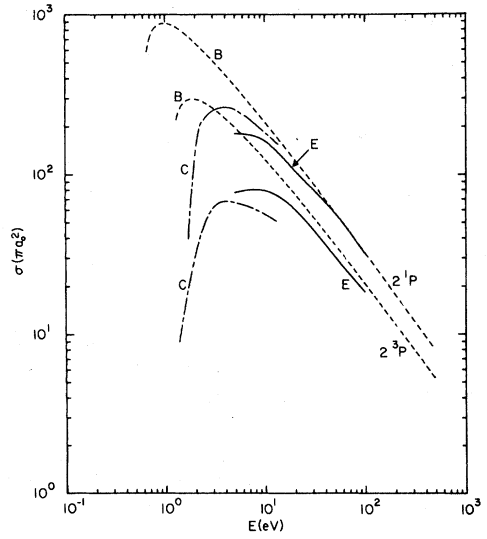

FIG. 1. Cross sections (πa_0^2) for the $2\,^{1,3}S$-$2\,^{1,3}P$ transitions induced in helium by electron impact at energy E (eV). E: Present multichannel eikonal treatment. B: Born approximation (Refs. 1, 10). C: Burke *et al.* (Ref. 11).

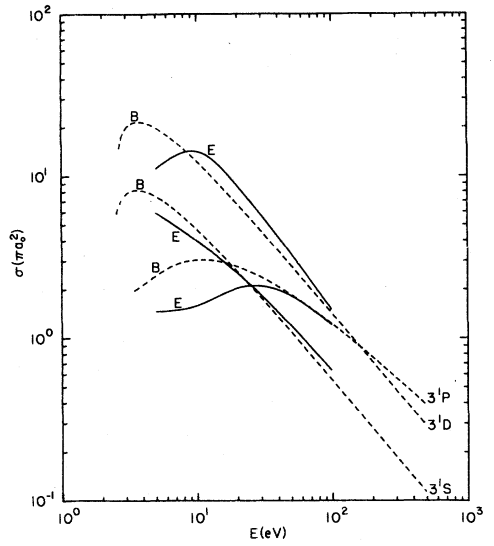

FIG. 2. Cross sections (πa_0^2) for the $2\,^1S$-$3\,^1S$, $3\,^1P$, $3\,^1D$ transitions induced in helium by electron impact at energy E (eV). E: Present treatment. B: Born approximation (Refs. 1, 10).

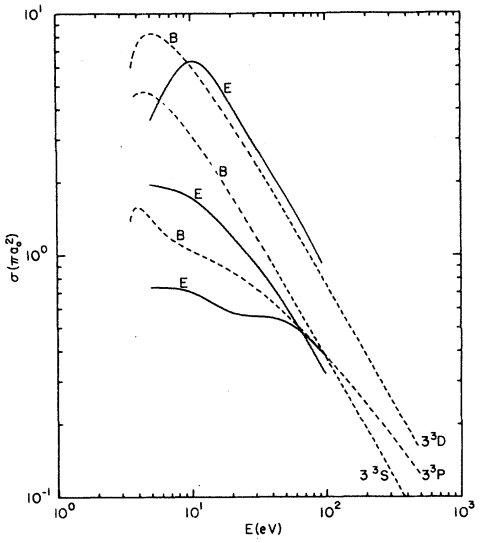

FIG. 3. Cross sections (πa_0^2) for the $2\,^3S$-$3\,^3S$, $3\,^3P$, $3\,^3D$ transitions induced in helium by electron impact at energy E (eV). E: Present treatment. B: Born approximation (Refs. 1, 10).

become greater than the $3\,^{1,3}S$ excitations. The results of Burke *et al.*,[11] who used simple analytic wave functions, closely coupled the $n=1$ and $n=2$ states for total (system) angular momentum $L=0$ and $L=1$, and used a Born approximation for higher L, are also displayed in Fig. 1 for comparison. A remarkable feature is that the Born limit is approached by the eikonal treatment at fairly low E, especially for the singlet transitions. Validity of Born's approximation has, as yet, not been fully explored for collisions involving excited atoms, although here the criterion $E \gg \epsilon_f - \epsilon_i$, the excitation energy, is satisfied for E much lower than that normally required for excitation from the ground state. The undulations in the $2\,^{1,3}S$-$3\,^{1,3}P$ cross sections in Figs. 2 and 3 are direct consequences of a zero in the corresponding form factors at nonzero momentum change K. In general, at low E, the stronger (optically forbidden) transitions are less affected by couplings than the weaker $2\,^{1,3}S$-$3\,^{1,3}P$ transitions which, however, converge more rapidly onto the Born limit at higher E.

The present ten-channel cross sections σ_M for excitation of magnetic sublevel M of (28) are displayed in Table I. Note that the cross sections $\sigma(nlm)$ for excitation of the $n\,^{1,3}P$ ($m=\pm1$) and $3\,^{1,3}D$ ($m=\pm2$) substates dominate the cross sections $\sigma(nl)$ for excitation of the respective levels (nl) at high impact energies. This behavior is consistent with the high-energy limit to Born's approximation, which predicts that the ratio $\sigma(nlm)/\sigma(nl)$ is $2|P_l^m(0)|^2/(2l+1)$, where the associated Legendre functions $P_l^m(0)$ are zero for odd $(l-m)$, and are largest when $|m|=l$. Alternatively, when impulsive conditions prevail, the change ΔL_y in the angular momentum perpendicular to the XZ scattering plane is directly proportional to the linear momentum change $K \approx 2k_i \sin\frac{1}{2}\theta$, which is perpendicular to the incident direction and which vanishes for high-energy scattering in the forward direction, thereby permitting angular momentum changes only in the Z direction to occur. Cross sections for the $2\,^1S$-$1\,^1S$ superelastic collision are also provided such that the detailed balance relation

$$k_i^2 \sigma_{if}(k_i) = k_f^2 \sigma_{fi}(k_f),$$
$$k_i^2 = k_f^2 + (2\mu/\hbar^2)(\epsilon_f - \epsilon_i) \tag{29}$$

between the forward and reverse rates for the process can be tested, thereby permitting assessment of the overall accuracy of the calculations. Thus, the crosses in Fig. 4 refer to the present $2\,^1S$-$1\,^1S$ results for the left-hand side of (29), with $E \geq 5$ eV, while the dots, representing the right-hand side of (29), are taken from a previous ten-channel treatment[4] of the $2\,^1S$ excitation from the ground state for $E \gtrsim 40$ eV. The maximum deviation corresponds to an error of 2.5% in σ.

The plane-polarization fractions[12]

TABLE I. Integral cross sections (πa_0^2) for the $2\,^1S$-$n\,^1L$ and $2\,^3S$-$n\,^3L$ transitions (S and T, respectively) in helium by collision with incident electrons of energy E (eV).

nL (m) \ E (eV)	S	T	S	T	S	T	S	T	S	T
	5		10		20		50		100	
$2P$ (0)	5.71^{1} [a]	3.07^{1}	4.01^{1}	2.38^{1}	1.02^{1}	1.29^{1}	9.94^{-1}	2.26	2.58^{-1}	1.64
$2P$ (±1)	1.23^{2}	4.63^{1}	1.22^{2}	5.53^{1}	9.51^{1}	4.70^{1}	5.63^{1}	2.81^{1}	3.16^{1}	1.67^{1}
$2P$ (Σ)	1.80^{2}	7.70^{1}	1.62^{2}	7.91^{1}	1.05^{2}	5.99^{1}	5.73^{1}	3.04^{1}	3.19^{1}	1.83^{1}
$3S$	5.92	1.95	3.99	1.72	2.52	1.20	1.19	6.18^{-1}	6.29^{-1}	3.21^{-1}
$3P$ (0)	1.08	6.42^{-1}	8.40^{-1}	3.78^{-1}	9.29^{-1}	2.38^{-1}	4.57^{-1}	2.60^{-1}	1.80^{-1}	2.00^{-1}
$3P$ (±1)	3.72^{-1}	9.48^{-2}	7.36^{-1}	3.24^{-1}	1.10	3.40^{-1}	1.36	2.68^{-1}	1.02	1.80^{-1}
$3P$ (Σ)	1.45	7.37^{-1}	1.58	7.02^{-1}	2.03	5.78^{-1}	1.82	5.28^{-1}	1.20	3.80^{-1}
$3D$ (0)	2.73	1.34	3.03	1.72	1.49	8.34^{-1}	4.69^{-1}	2.81^{-1}	2.34^{-1}	2.17^{-1}
$3D$ (±1)	6.56	1.89	7.16	3.20	3.58	1.81	8.96^{-1}	6.35^{-1}	2.29^{-1}	2.51^{-1}
$3D$ (±2)	1.78	3.87^{-1}	3.89	1.40	3.52	1.45	1.92	8.55	1.02	5.41^{-1}
$3D$ (Σ)	1.11^{1}	3.62	1.41^{1}	6.32	8.59	4.09	3.28	1.77	1.48	1.01
$1\,^1S$	1.47^{-1}	...	8.63^{-2}	...	5.06^{-2}	...	2.91^{-2}	...	1.72^{-1}	...

[a] Exponents indicate the power of 10 by which the entry is to be multiplied.

$$P(n\,^1P\text{-}n\,^1S)=\frac{\sigma_0-\sigma_1}{\sigma_0+\sigma_1}, \tag{30a}$$

$$P(n\,^3P\text{-}2\,^3S)=\frac{15(\sigma_0-\sigma_1)}{41\sigma_0+67\sigma_1}$$

and

$$P(3\,^1D\text{-}2\,^1P)=\frac{3(\sigma_0+\sigma_1-2\sigma_2)}{5\sigma_0+9\sigma_1+6\sigma_2}, \tag{30b}$$

$$P(3\,^3D\text{-}n\,^3P)=\frac{213(\sigma_0+\sigma_1-2\sigma_2)}{671\sigma_0+1271\sigma_1+1058\sigma_2}$$

for the dipole radiation emitted from the excited states are presented in Table II. The effect of the couplings on the magnetic substates is strongly evident, particularly for the P-S transitions, when little correspondence is exhibited between columns 2 and 4 and between 3 and 5.

A. Differential cross sections

In Fig. 5 are displayed the differential cross sections for the singlet-singlet transitions, as a function of scattering angle θ and impact energy E (eV). The structure present in the $3\,^1P$ excitation but absent in the $2\,^1P$ excitation is a direct consequence of the very important, strong $3\,^1D(m=0,\pm1,\pm2)$-$3\,^1P$ close couplings which affect the magnetic substates of $3\,^1P$ more than do the ^1P-^1S couplings. The relative importance of close encounters (large-angle scattering) for optically forbidden vs optically allowed transitions is exhibited by the slower decrease with θ in Figs. 5(b) and 5(d) relative to that in Figs. 5(a) and 5(c).

No measurements or other theoretical calculations are available. However, since excitation from the $1\,^1S$ state was very well described (when compared with experiment) by the multichannel eikonal approach for $0\lesssim\theta\lesssim40°$, a range contributing effectively all of the integral cross section, the data in Fig. 5 are presumed quite accurate for small-angle scattering. Electron-exchange effects, important for large-angle scattering,[4] have been

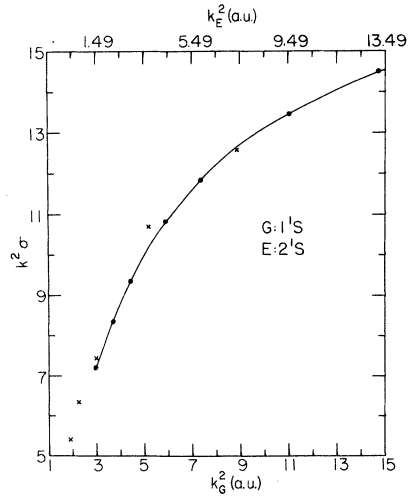

FIG. 4. Test of detailed balance between the forward and reverse rates of the $1\,^1S$-$2\,^1S$ collisional excitation in helium by electrons with wave number k_G and k_E in the $1\,^1S$ and $2\,^1S$ channels, respectively. ●: Previous $\sigma(1\,^1S$-$2\,^1S)$ data (Ref. 4). ×: Present $\sigma(2\,^1S$-$1\,^1S)$ data.

TABLE II. Polarization fractions of radiation of wavelength λ (Å) emitted from the collisionally excited states n' to state n.

n'-n / λ (Å) / E (eV)	$2\,^1P$-$n\,^1S$ 20581(2) [a] 584(1)	$2\,^3P$-$2\,^3S$ 10830	$3\,^1P$-$n\,^1S$ 5016(2) 537(1)	$3\,^3P$-$2\,^3S$ 3889	$3\,^1D$-$2\,^1P$ 6678	$3\,^3D$-$2\,^3P$ 5876
5	−0.037	0.040	0.706	0.302	0.262	0.175
10	−0.207	−0.020	0.391	0.123	0.138	0.104
20	−0.647	−0.076	0.256	0.048	−0.021	0.025
50	−0.932	−0.171	−0.196	0.096	−0.248	−0.052
100	−0.968	−0.161	−0.478	0.116	−0.383	−0.072

[a] Value of lower-level n in parenthesis.

explicitly neglected, although some (small) allowance does result by virtue of a multistate target expansion. Also differential cross sections for excitation of the m substates are available from the authors. No measurements exist as yet, although when various theoretical and experimental data for the $1\,^1S$-$2\,^1P_0$ differential magnetic sublevel cross sections were compared for electron-helium scattering at 60 and 80 eV, Chutjian and Srivastava[13] concluded that the corresponding multichannel eikonal treatment provided the best agreement with their recent measurements.

Cross sections obtained for the corresponding triplet-triplet transitions are smaller than and demonstrate behavior similar to that in Fig. 5. They are available from the authors upon request.

B. Angular correlation parameters and circular polarization fractions

In Figs. 6(a) and 6(b) are presented graphical displays, as functions of θ and E, of λ, the relative contribution to the differential cross section arising from ^1P ($m=0$) scattering, and of χ, the phase difference between the ^1P dipoles oscillating ($m=0$) and rotating ($m=\pm1$) about the Z axis. Forward ($\theta\approx0$) and large-angle ($\theta\gtrsim40°$) inelastic scattering is mainly in the $m=0$ channel, with $m=\pm1$ excitations being dominant at the intermediate angles. As E is decreased, this intermediate angular range increases, and the range for $m=0$ scattering in the forward direction also increases, although not as rapidly.

The $2\,^1P$ phase difference χ in Fig. 5(b) is negative for all θ and passes through $-\frac{1}{2}\pi$ twice for all E, and $-\pi$ twice only for the lowest $E\sim5$ eV. This behavior assumes significance in the fraction of circularly polarized radiation emitted from the $2\,^1P$ states. Thus, provided the populations of the $m=0$ and ±1 sublevels are equal (i.e., $\lambda\approx0.5$), then $\Pi=-\sin\chi$; fully circularly polarized light is observed when $\chi\approx-\frac{1}{2}\pi$, and is absent when $\chi\approx-\pi$ at two scattering angles θ. Figure 5(a), however shows that the $m=0$ and $m=\pm1$ substates are not equally populated, in general, except at specific θ, and the combined effect of phase difference and departure from equal populations is exhibited in Fig. 6 which displays Π given by (17) as a function of θ and E. This figure shows that circularly polarized light is observed when the electrons are scattered through fairly large angles which decrease as E increases. Moreover, Π passes through zero twice, only for $E=5$ eV, as expected from Fig. 5(b). Figure 7 also provides the angular momentum (17) transferred at right angles to the scattering plane, and hence the maxima, almost reaching unity, correspond to the transfer of ~1 unit of angular momentum ($\hbar$) to the atom which is therefore left in the $m=0$ state.

Similar graphical displays of λ, χ, and Π have been obtained for the remaining transitions (and are available from the authors). No experimental data exist. However, a corresponding ten-channel treatment[4] of the $1\,^1S$-$2\,^1P$, $3\,^1P$ transitions in helium by electron impact resulted in satisfactory agreement with the recent λ, χ measurements of Eminyan *et al.*[8]

Finally, the effect of the neglect of electron exchange and of couplings with channels $n\geq4$ is difficult to assess without resort to more detailed and elaborate calculations. For transitions from the $1\,^1S$ state, electron exchange is effective only for the close encounters resulting in large-angle scattering. These large angles, however, provide negligible contribution to the inelastic integral cross sections,[4,14] which are determined solely by scattering mainly in the forward direction ($\theta\lesssim20°$) at intermediate impact energies. Also, explicit inclusion[1] of exchange within the the VPS approximation for e-He($2\,^{1,3}S$) collisions causes little change for $E\gtrsim10$ eV. A better representation of the direct scattering function is apparently more important and is obtained by the present inclusion of close couplings.

We note that a fully quantal close-coupling cal-

culation would in practice be prohibitively difficult in that an extremely large number of angular momentum states L of relative motion are distorted by the strong dipole interactions evident in the present study. Thus, the normal procedure of performing fully quantal computations for $L=0 \rightarrow L_{\max} \sim 10$ and a Born approximation for $L>10$ simply will not suffice, since the present investigation has shown that impact parameters $\rho \sim 100$ a.u. ($\equiv L/k_i$) are influenced appreciably by the

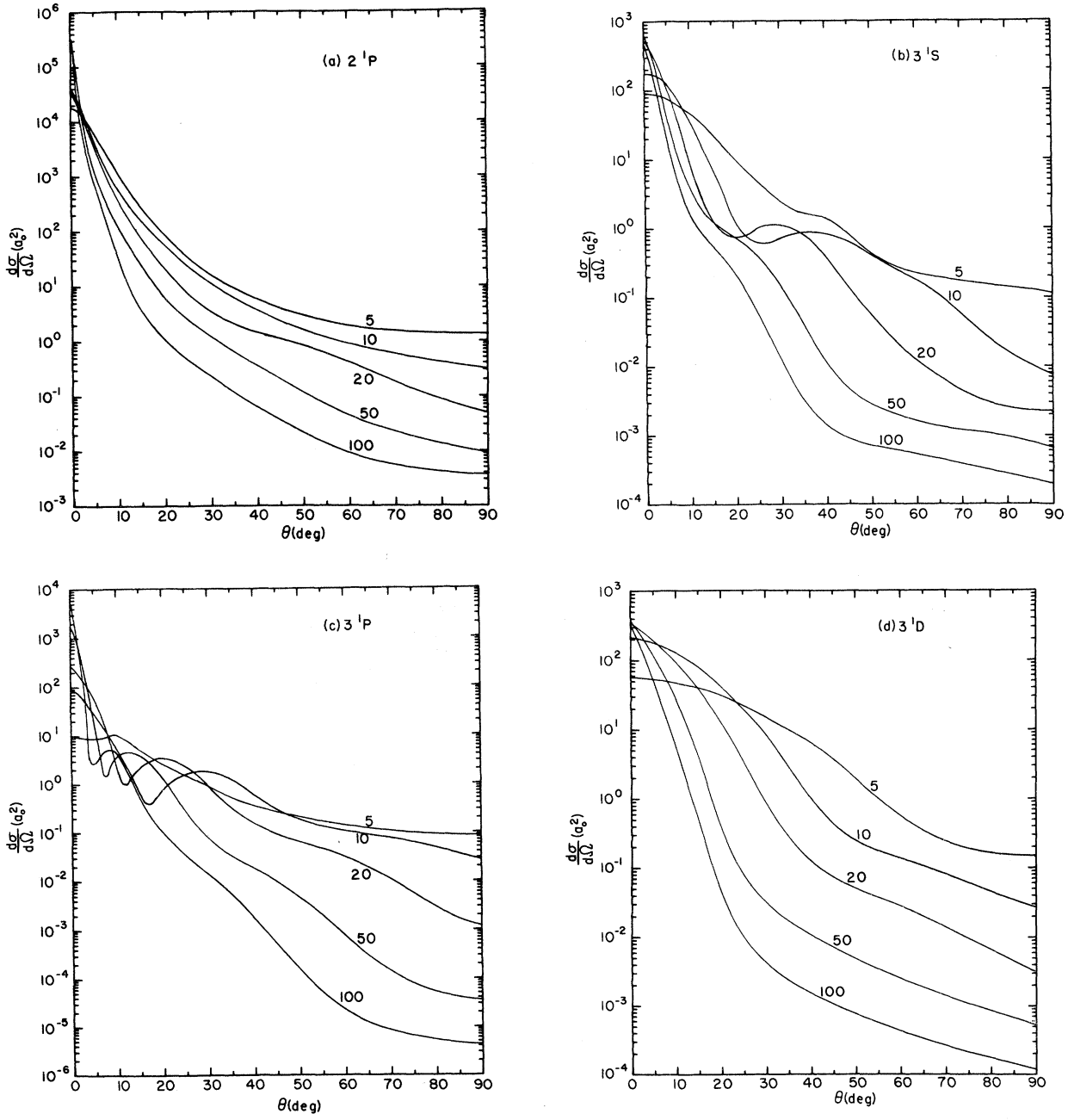

FIG. 5. Differential cross sections (a_0^2/sr) as a function of scattering angle θ (deg) and impact energy E (eV) indicated on each curve for (a) $2\,^1P$, (b) $3\,^1S$, (c) $3\,^1P$, and (d) $3\,^1D$ excitations, summed over final magnetic substates m.

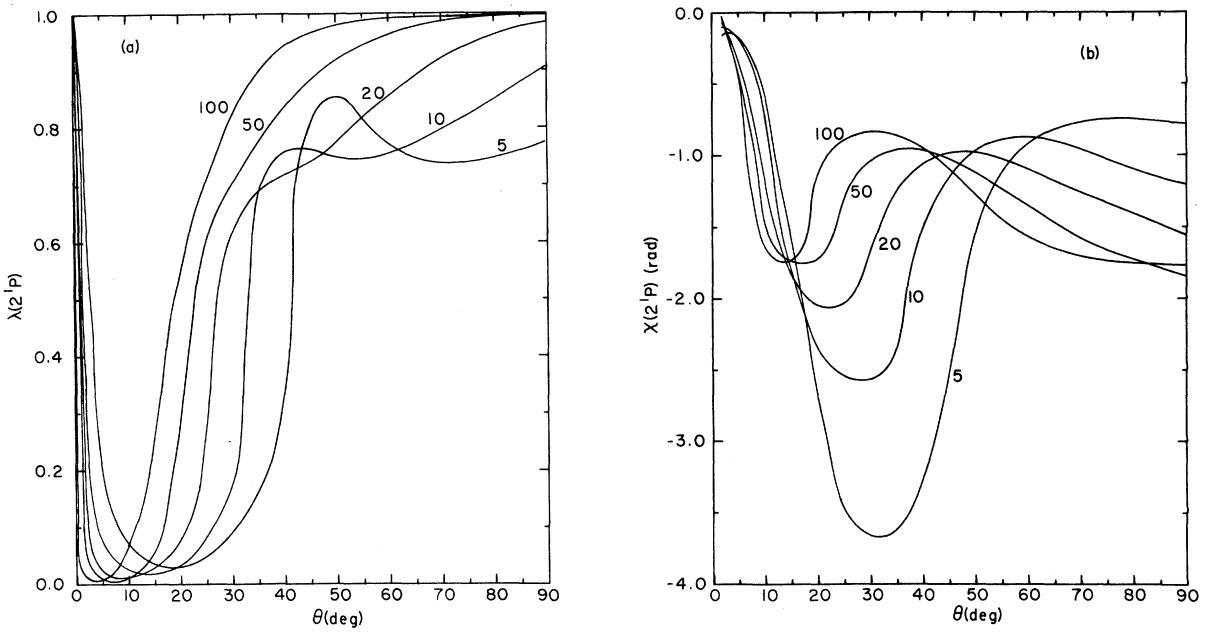

FIG. 6. Variation of (a) $\lambda(2\,^1P)$ and (b) $\chi(2\,^1P)$ with electron-scattering angle θ (deg) and with electron impact energy E (eV) indicated on each curve.

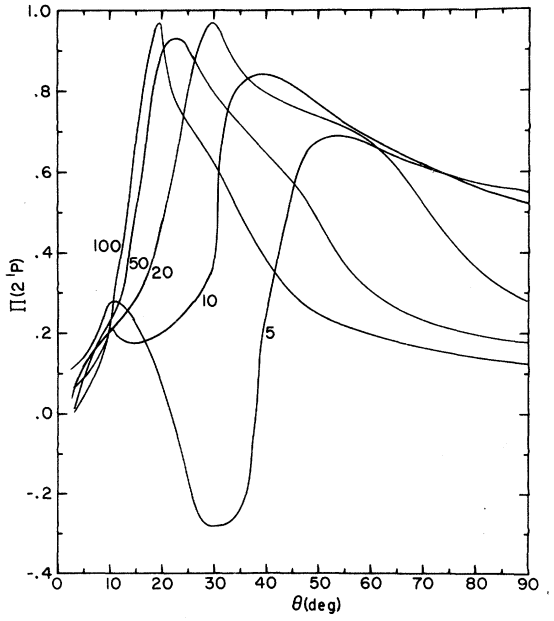

FIG. 7. Variation of the fraction Π of circularly polarized radiation, emitted from $He(2\,^1P)$ and observed perpendicular to the scattering plane, with electron-scattering angle θ and impact energy E (eV) indicated on each curve.

various distortions. The advantage of the present treatment is that the multichannel eikonal expression (18) ensures that convergence in partial-wave contributions is always attained without undue difficulty, especially in the high-energy limit, and that the long-range couplings have a mechanism whereby they can affect distant encounters (or large L) important to the processes investigated here.

In conclusion, for e-$He(2\,^{1,3}S)$ inelastic collisions at impact energies $E \leq 100$ eV, couplings with the neighboring $n=2$ and 3 levels are important, particularly those involving the $3\,^{1,3}D$ states, the excitations of which dominate transitions to the $n=3$ level at low E. The Born limit is approached at energies (~100 eV for singlet-singlet transitions) lower than those normally in evidence for excitation from ground states. Detailed balance between the forward and reverse rates of the $2\,^1S \rightleftarrows 1\,^1S$ transitions is satisfied. The competition between the relative populations λ of the magnetic P substates and the phases χ of the corresponding excitations is exhibited by the variation of Π, the fraction of circularly polarized radiation emitted from these P states, with impact energy E and scattering angle θ.

*Research sponsored by the Air Force Aerospace Research Laboratories, Air Force Systems Command, U. S. Air Force Contract No. F33651-74-C-4003.

[1]M. R. Flannery, W. F. Morrison, and B. L. Richmond, J. Appl. Phys. 46, 1186 (1975).

[2]M. R. Flannery and K. J. McCann, J. Phys. B 7, 2518 (1974); 7, L522 (1974).

[3]K. J. McCann and M. R. Flannery, Phys. Rev. A 10, 2264 (1974).

[4]M. R. Flannery and K. J. McCann, J. Phys. B (to be published).

[5]M. Cohen and R. P. McEachran, Proc. Phys. Soc. 92, 37 (1967); J. Phys. B 2, 1271 (1969); additional coefficients not tabulated in these references were obtained by private communication (1974).

[6]L. I. Schiff, Phys. Rev. 103, 443 (1956).

[7]E. Gerjuoy and B. K. Thomas, Rep. Prog. Phys. 37, 1345 (1974).

[8]M. Eminyan, K. B. MacAdam, J. Slevin, and H. Kleinpoppen, J. Phys. B 7, 1519 (1974).

[9]U. Fano and J. H. Macek, Rev. Mod. Phys. 45, 533 (1973).

[10]Y-K. Kim and M. Inokuti, Phys. Rev. 181, 205 (1969). The authors wish to thank Dr. Y-K. Kim for sending us detailed tables of the form factors which were only partially given in this reference.

[11]P. G. Burke, J. W. Cooper, and S. Ormonde, Phys. Rev. 183, 245 (1969).

[12]I. C. Percival and M. J. Seaton, Philos. Trans. R. Soc. Lond. A 251, 113 (1958).

[13]A. Chutjian and S. K. Srivastava, J. Phys. B (to be published).

[14]D. H. Madison and W. N. Shelton, Phys. Rev. A 7, 499 (1973).